RESEARCH ARTICLE

Analysis of Three μ1-AP1 Subunits During Zebrafish Development

Giuseppina Gariano,[1] Michela Guarienti,[2] Roberto Bresciani,[2] Giuseppe Borsani,[3] Giulia Carola,[2] Eugenio Monti,[2] Roberta Giuliani,[2] Rita Rezzani,[4] Francesca Bonomini,[4] Augusto Preti,[2] Peter Schu,[5]* and Daniela Zizioli[2]*

Background: The family of AP-1 complexes mediates protein sorting in the late secretory pathway and it is essential for the development of mammals. The ubiquitously expressed AP-1A complex consists of four adaptins γ1, β1, μ1A, and σ1A. AP-1A mediates protein transport between the trans-Golgi network and early endosomes. The polarized epithelia AP-1B complex contains the μ1B-adaptin. AP-1B mediates specific transport of proteins from basolateral recycling endosomes to the basolateral plasma membrane of polarized epithelial cells. Results: Analysis of the zebrafish genome revealed the existence of three μ1-adaptin genes, encoding μ1A, μ1B, and the novel isoform μ1C, which is not found in mammals. μ1C shows 80% sequence identity with μ1A and μ1B. The μ1C expression pattern largely overlaps with that of μ1A, while μ1B is expressed in epithelial cells. By knocking-down the synthesis of μ1A, μ1B and μ1C with antisense morpholino techniques we demonstrate that each of these μ1 adaptins is essential for zebrafish development, with μ1A and μ1C being involved in central nervous system development and μ1B in kidney, gut and liver formation. Conclusions: Zebrafish is unique in expressing three AP-1 complexes: AP-1A, AP-1B, and AP-1C. Our results demonstrate that they are not redundant and that each of them has specific functions, which cannot be fulfilled by one of the other isoforms. Each of the μ1 adaptins appears to mediate specific molecular mechanisms essential for early developmental processes, which depends on specific intracellular vesicular protein sorting pathways. *Developmental Dynamics 243:299–314, 2014.* © 2013 Wiley Periodicals, Inc.

Key words: adaptin; central nervous system; development; vesicular transport; kidney; zebrafish

Key findings:

- Zebrafish genome hosts three genes encoding for μ1-adaptin subunits. μ1A, μ1B evolutionary conserved and the novel μ1C.
- The μ1C expression pattern largely overlaps with that of μ1A, while μ1B is expressed in epithelial cells
- Morpholino approach demonstrates that μ1 adaptin subunits are essential for development

Submitted 20 May 2013; First Decision 25 September 2013; Accepted 27 September 2013

INTRODUCTION

The family of the heterotetrameric adaptor-protein complexes comprises the five members AP-1, AP-2, AP-3, AP-4, and AP-5 (Hirst et al., 2011, 2013). AP-2 mediates clathrin-dependent endocytosis, whereas the other complexes mediate vesicular protein sorting in endosomal pathways. The ubiquitous AP-1A complex is formed by the adaptins γ1, β1, μ1A and σ1A. AP-1 adaptin isoforms with tissue-specific expression exist, which share the γ1 and β1 subunits. A mouse knockout of γ1-adaptin ceases

[1]Unit of Experimental Oncology and Immunology, Department of Molecular and Translational Medicine University of Brescia, Italy
[2]Unit of Biotechnology, Department of Molecular and Translational Medicine University of Brescia, Italy
[3]Unit of Biology and Genetic, Department of Molecular and Translational Medicine University of Brescia, Italy
[4]Unit of Anatomy and Physiopathology, Department of Clinical and Experimental Sciences, University of Brescia
[5]Center for Biochemistry and Molecular Cell Biology, Inst. for Cellular Biochemistry, Georg-August University, Göttingen, Germany
Grant sponsor: Fondazione CARIPLO to G.B.; Grant sponsor: ZebraGene.; Grant sponsor: DFG to P.S.; Grant number: Schu 802/3-2.
***Correspondence to: Daniela Zizioli, Unit of Biotechnology, Department of Molecular and Translational Medicine University of Brescia, Viale Europa 11, 25123 Brescia, Italy. E-mail: zizioli@med.unibs.it and Peter Schu, Cellular Biochemistry, University Göttingen. E-mail: pschu@gwdg.de**

DOI: 10.1002/dvdy.24071
Published online 7 October 2013 in Wiley Online Library (wileyonlinelibrary.com).

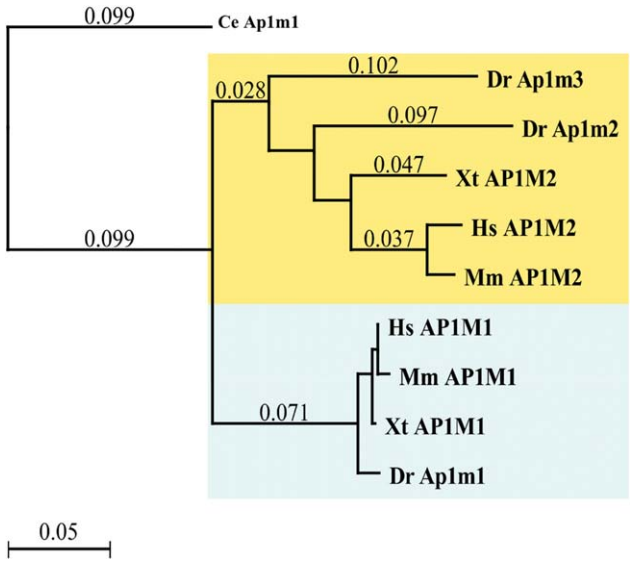

Fig. 1. Phylogenetic tree of vertebrate μ-1 adaptins. Unrooted tree showing the phylogenetic analysis for human (Hs), mouse (Mm), *Xenopus* (Xt), and zebrafish (Dr) μ1-adaptin subunits. The Ce Ap1m1 polypeptide from *Caenorhabditis elegans* has been used as outgroup sequence. The horizontal bar represents a distance of 0.05 substitutions per site.

development at the blastocyst stage, demonstrating essential functions of AP-1 in development (Zizioli et al., 1999). A mouse μ1A knockout ceases development later, at mid-organogenesis, due to the expression of the epithelia specific isoform μ1B (Ohno et al., 1999; Meyer et al., 2000). In addition to σ1A, vertebrates express the tissue-specific isoforms σ1B and σ1C and most tissues express σ1A and just one of the two isoforms. AP-1/σ1B is involved in the apical synaptic vesicle recycling pathway and its deficiency leads to severely impaired learning and memory (Glyvuk et al., 2010). σ1A-deficiency leads to severe developmental defects and peri-natal lethality in humans whereas zebrafish knockdown is viable (Montpetit et al., 2008). Adaptins fulfil specific functions in AP-1-dependent protein sorting. γ1 and β1 mediate clathrin recruitment and Arf-1 binding. μ1 adaptins mediate binding of cargo proteins containing tyrosine-based sorting motifs, whereas the γ1/σ1A hemicomplex binds cargo proteins containing leucine-based sorting motifs (Boehm and Bonifacino, 2001). γ1 and μ1A are both involved in the regulation of AP-1 membrane binding. γ1 is predicted to bind the phospholipid PI-4-P and thus mediates AP-1 membrane targeting (Wang et al., 2003). μ1A is involved in the regulation of AP-1 membrane-cytoplasm recycling (Medigeshi et al., 2008; Radhakrishnan et al., 2013). The μ1A knockout in mouse leads to the absence of both AP-1 complexes expressed in brain, AP-1/σ1A and AP-1/σ1B. These embryos show most severe defects in brain development. Angiogenesis is not detectable and they show severe hemorraghes in the ventricles and spinal canal (Meyer et al., 2000). AP-1/σ1B knockout mice are viable, demonstrating that the AP-1/σ1A complex is indispensable for brain development (Glyvuk et al., 2010). In the AP-1B complex, μ1B mediates binding of the complex to basolateral recycling endosomes from which it transports cargo to the basolateral plasma membrane. AP-1A mediates basolateral sorting at the trans-Golgi network, but both complexes can partially compensate the deficiency of the other (Eskelinen et al., 2002; Zizioli et al., 2010; Gravotta et al., 2012). Recently proteins have been identified being sorted basolateral/dendritic by AP-1A in neurons (Farias et al., 2012). μ1B-deficient mice are viable, but they have impaired gut formation and they are smaller. Deficiencies in kidney function, the tissue with highest μ1B expression, have not been reported (Takahashi et al., 2011). In contrast, μ1B knockdown in zebrafish impairs gut and pronephritic duct development. Importantly, we showed that μ1B is also expressed in zebrafish liver, in contrast to the mouse orthologue, and that μ1B is essential for zebrafish liver development (Zizioli et al., 2010).

How do μ1A and μ1B fulfil their specific functions? μ1 adaptins consist of an 150 aa long N-terminal globular domain and 275 aa long C-terminal domain. The cargo protein binding domain is formed by residues in the C-terminal domain and these are conserved in μ1A and μ1B, which indicates that they bind the same set of transmembrane proteins and indeed, they can partially substitute each other in basolateral protein sorting (Eskelinen et al., 2002; Zizioli et al., 2010; Carvajal-Gonzalez et al., 2012). μ1B targets the AP-1B to recycling endosomes by means of its PIP_3 binding motif, which is formed by residues in the C-terminal domain (Folsch et al., 2001), whereas AP-1A membrane targeting requires PI-4-P, most likely recognized by means of a domain in γ1 (Wang et al., 2001; Heldwein et al., 2004). The N-terminal domain of μ1A is involved in regulating membrane-cytoplasma recycling, by means of binding the cytoplasmic effector protein prolyl-endopeptidase-like protein (PREPL). Disturbed AP-1A recycling leads to protein missorting and an altered trans-Golgi network morphology (Medigeshi et al., 2008; Radhakrishnan et al., 2013). We used zebrafish to study the evolutionary conservation and functions of μ1 adaptins and AP-1 complexes during vertebrate development and discovered a third μ1 adaptin in zebrafish, μ1C. We demonstrate that, like μ1A, μ1C is expressed in the central nervous system, but despite a high sequence homology and a large overlap in their expression pattern they are not-redundant. In addition we refined our analysis of specific functions of μ1B during zebrafish development.

RESULTS

In Silico Analysis of Zebrafish μ1-adaptins

The two AP-1 μ1-adaptins, μ1A and μ1B, have been described and analyzed in mammals (Boehm and Bonifacino, 2001; Ohno, 2006). We already described the two zebrafish genes, *ap1m1* and *ap1m2*, representing orthologs of the mammalian

TABLE 1. Main features of zebrafish μ1 adaptins

zebrafish μ subunits	gene	locus	gene organization	protein
μ1A	ap1m1 (ORF 1269 bp)	Chr 2	12 ex – 11 int	Ap1m1 (423 aa)
μ1B	ap1m2 (ORF 1272 bp)	Chr 6	12 ex – 11 int	Ap1m2 (424 aa)
μ1C	ap1m3 (ORF 1269 bp)	Chr 6	12 ex – 11 int	Ap1m3 (423 aa)

counterparts (Zizioli et al., 2010). *ap1m2* expression analysis revealed a specific μ1B (Ap1m2) expression in polarized epithelia cells, but in contrast to mammals, μ1B was found to be expressed in zebrafish liver, pointing to specific differences in liver development between teleosts and mammals. Recently, we performed a new bioinformatic analysis using both the TBLASTN and BLAST algorithms against the latest zebrafish assembly of genomic sequences (Zv9) and this led to the identification of a third gene *ap1m3*. Following the Zebrafish Nomenclature Committee Guidelines (www.zfin.org), the novel gene was named *ap1m3* (access no. NM_001114441) and the protein μ1C (Fig. 1). While *ap1m1* is located on chromosome 2, *ap1m2* and *ap1m3* are both located on chromosome 6 (Table 1). The exon-intron structure of all the zebrafish genes is similar (12 exons, 11 introns) and also to the human genes for μ1A and μ1B (Nakatsu et al., 1999). The presence of extra gene paralogs in zebrafish is a relatively a common finding that has been extensively documented, and is mostly due to an additional round of genome duplication. This suggests that *ap1m1*, *ap1m2*, and *ap1m3* may have originated from a genomic duplication which took place during evolution of the teleost line (Postlethwait et al., 1998). The encoded proteins also show highly conserved primary structures. The μ1C polypeptide is 423 amino acids long (access no. NP_001107913) showing 80% amino acid sequence identity to μ1A and μ1B (Table 2). Sequence alignment of the three zebrafish proteins shows that residues exist, which are not conserved in either isoform and that others are conserved between C and A or between C and B isoforms (Fig. 2). The nonconserved residues are also not found in μ-adaptins of AP-2, −3, or −4 indicating that they may indeed fulfil AP-1 complex specific functions. The crystal structure of μ1A has been solved as a part of an AP-1 complex (Heldwein et al., 2004). We modelled the structures of all three zebrafish μ1-adaptins on the mammalian μ1A (zebrafish μ1A 98% sequence identity) and marked the nonconserved and thus isoform specific residues of A, B, and C (Fig. 3). These are not distributed randomly, but are clustered in domains facing the β1-adaptin. The N-terminal amino acids (1–150) form a globular domain, which mediates binding to β1 adaptin and thus contributes to β1/μ1 hemi-complex formation (Collins et al., 2002; Heldwein et al., 2004). The first eighty amino acids of this domain are less conserved (25%) and this μ1A domain is involved in the regulation of AP-1 membrane-cytoplasm recycling (Medigeshi et al., 2008; Radhakrishnan et al., 2013). This domain is not in contact with the membrane, is accessible from the cytoplasmic face of the complex and binds the N-terminal domain of PREPL (prolyl-endopeptidase-like protein). PREPL-deficiency leads to an increased TGN pool of AP-1 and a dramatically enlarged TGN (Radhakrishnan et al., 2013). The corresponding domain of μ1B may also be involved in the regulation of AP-1B recycling, because antibodies directed against this domain impair AP-1B recycling, but not in all cell lines (Cancino et al., 2007). This indicates that the isoforms evolved primarily to allow pathway-specific regulation of AP-1 membrane binding. The other specific residues are clustered in two regions in the C-terminal, cargo protein binding domain (Fig. 3). This domain has to flip out of the core complex to make the cargo binding motif accessible and to move it closer toward the membrane. It is not known, whether this domain of μ1A contains residues mediating specific interactions with membrane lipids, as it has been shown for μ1B (PIP_3, recycling endosomes) and μ2 (PI-4,5-P_2, plasma membrane) (Collins et al., 2002; Krauss et al., 2006; Fields et al., 2010). The fact that all three zebrafish μ1 adaptins have two clusters of nonconserved residues in this domain indicates

TABLE 2. Percentage of identity (bold values) and similarity (regular values)

	Dr Ap1m3	Dr Ap1m2	Xt AP1M2	Mm AP1M2	Hs AP1M2	Dr Ap1m1	Xt AP1M1	Mm AP1M1	Hs AP1M1
Dr Ap1m3	**100.0**	**79.0**	**80.1**	**79.4**	**78.5**	**78.7**	**79.2**	**78.7**	**79.0**
Dr Ap1m2	89.4	**100.0**	**83.7**	**83.5**	**82.5**	**76.9**	**76.4**	**76.2**	**76.4**
Xt AP1M2	91.5	94.3	**100.0**	**90.3**	**89.8**	**81.1**	**80.6**	**80.1**	**80.4**
Mm AP1M2	89.4	93.6	96.9	**100.0**	**96.9**	**80.1**	**80.1**	**79.7**	**79.9**
Hs AP1M2	88.7	92.9	96.2	98.6	**100.0**	**79.9**	**80.1**	**79.4**	**79.7**
Dr Ap1m1	89.8	90.6	92.7	91.3	90.8	**100.0**	**98.1**	**97.2**	**97.9**
Xt AP1M1	89.8	90.3	92.7	91.5	91.0	99.8	**100.0**	**98.8**	**99.5**
Mm AP1M1	89.8	90.6	92.7	91.7	90.8	99.5	99.8	**100.0**	**99.3**
Hs AP1M1	89.8	90.6	92.7	91.7	90.8	99.5	99.8	100.0	**100.0**

Fig. 2. Sequence alignment of the three zebrafish μ1-adaptins. Multiple alignment of amino acid sequences of zebrafish adaptins: *Dr* Ap1m1 (μ1A), *Dr* Ap1m2 (μ1B), *Dr* Ap1m3 (μ1C) performed using the ClustalW algorithm. Red bars indicate percentage conservation.

that all the C-terminal μ1 domains contribute to the regulation of AP-1 membrane binding, either directly by binding to specific membrane lipids or to other proteins. To identify μ1-adaptin specific AP-1 functions in development, we analyzed the μ1 expression patterns and reduced their expression.

μ1 Adaptin Expression During Zebrafish Development

Gene duplication is often followed by functional specification and therefore divergence in temporal and spatial expression. Expression analysis of μ1-adaptins in mammals revealed an ubiquitous expression of μ1A and a μ1B expression restricted to polarized epithelia (Ohno et al., 1999). We already demonstrated that in zebrafish, in addition to polarized epithelia, μ1B (Ap1m2) is also expressed in liver (Zizioli et al., 2010). Because of this difference in μ1B tissue-specificity and the presence of a third isoform, we tested the expression pattern of the novel Ap1m3 (μ1C) as well as that of Ap1m1 (μ1A) and Ap1m2 (μ1B). Temporal expression was analyzed by reverse transcriptase-polymerase chain reaction (RT-PCR) at different developmental stages, from 2-cells stage to 72 hours postfertilization (hpf) as well as in adult organs. Semiquantitative expression analysis by RT-PCR revealed the presence of the three transcripts at the zygote and 50% epiboly developmental stage, indicating that all the μ1-adaptin genes are maternally expressed. *ap1m1* and *ap1m3* transcripts show very similar expression patterns in each of the development stages analyzed (data not shown). The *ap1m1* transcript is expressed in all adult organs analyzed and appears to be most abundant in brain. Also

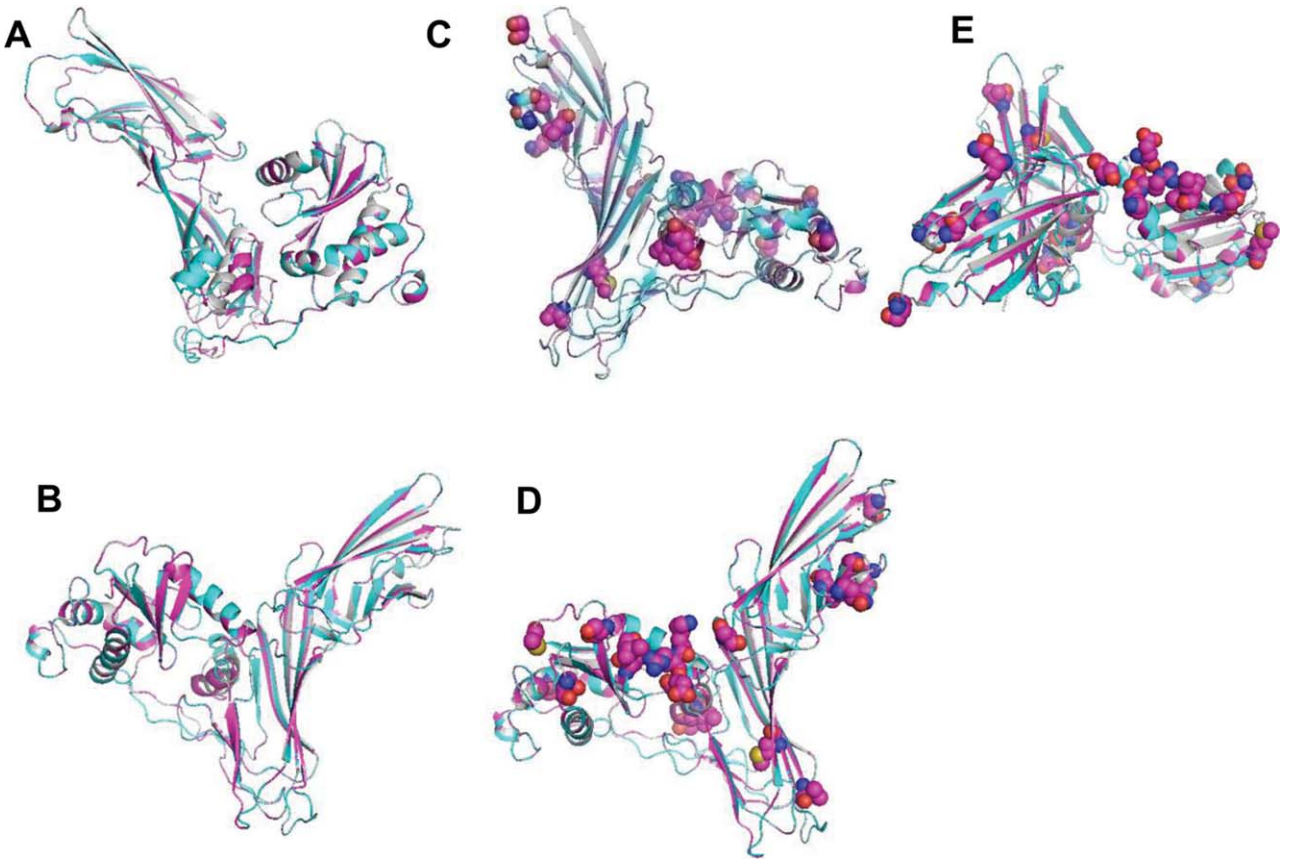

Fig. 3. Comparison of zebrafish μ1-adaptin structures. Overlay of zf μ1A (gray), μ1B (cyan), and μ1C (pink) structures, which are modelled on mammalian μ1A (Swiss modeler). **A,C,E:** the N-terminal globular domain is positioned to the right and the C-terminal domain to the left. **B,D:** structures shown in A and C rotated by 180°. 3D-structures are identical, with the exception of the position of a helix at the start of the C-terminal domain (aa 224–230), best seen in A. C,D,E: Residues not conserved in either isoform are shown as spheres of the respective μ1C residues. E: Top-view of the proteins showing the clustering of nonconserved residues in the N-terminal domain to the side close to β1-adaptin, which would be positioned above the μ1-adaptins.

the novel *ap1m3* transcript shows expression in all tissues and in particular in brain tissues. *ap1m2* expression is highest in gut, kidney, and liver, confirming previously published data, while there is no detectable expression in brain and muscle (Zizioli et al., 2010).

The spatial distribution of μ1-adaptin mRNAs has been further examined through whole-mount in situ hybridization (WISH) from the early stages of development to 48 hpf with digoxigenin-UTP-labeled probes. The WISH experiments confirmed the maternal expression of the three genes. At the 18 somites stage, a first divergence in spatial expression was evident among *ap1m1*, *ap1m2* and *ap1m3* genes. *ap1m2* is highly expressed in the caudal region, where gut and pronephritic ducts will develop while *ap1m1* and *ap1m3* were found particularly expressed in the rostral region of the embryos (data not shown). In Table 3 we summarized the expression pattern of the three adaptin genes. At 24 hpf, *ap1m1* is mainly expressed in the central nervous system (CNS), particularly at the hindbrain, midbrain and cerebellum regions (Fig. 4A:a–c). CNS restricted expression of *ap1m1* is maintained at 48 hpf (Fig. 4A:d). The *ap1m3* transcript also shows high expression in brain regions; with a clear labeling of cerebellum, hindbrain and midbrain at 24 hpf (Fig. 4C:a–c). In addition, at this developmental stage, a faint label at somite structures is present. At 48 hpf, expression of *ap1m3* is reduced and restricted to CNS regions (Fig. 4C:d) and is still detected in somites. As described in Table 3 and in a previous study (Zizioli et al., 2010), *ap1m2* expression is specifically restricted to gut region (intestinal bulb), pronephritic ducts and liver at 24 and 48 hpf. (Fig. 4B:a–d). Taken together, these data indicate that, starting from 24 hpf *ap1m1* and *ap1m3* are widely expressed in the brain of developing embryos. Although both shared a similar expression pattern in the midbrain, hindbrain and midbrain–hindbrain boundary, only *ap1m3* expression is detected in somites. These data demonstrate that zebrafish Ap1m1 (μ1A) expression is comparable to μ1A expression in mammals and that the novel Ap1m3 (μ1C) is likewise widely expressed, also with highest expression in brain. The latter finding is somehow unexpected, because adaptin isoforms analyzed so far show a tissue specific expression pattern and they fulfil tissue-specific functions.

μ1 Isoform Functions in Brain and Kidney Development

We performed loss-of-function studies of the three genes with antisense

TABLE 3. Tissue Specific Gene Expression at Different Developmental Stages[a]

	Tissue	*ap1m1*MO	*ap1m2*MO	*ap1m3*MO
24 hpf	CNS	+++	−	+++
	GUT	−	+++	−
	SOMITES	−	−	+
	PRONEPHRITIC DUCTS	−	+++	−
48 hpf	CNS	+++	−	+++
	GUT	−	+++	−
	SOMITES	−	−	++
	LIVER	−	+++	−
	PRONEPHRITIC DUCTS	−	+++	−

[a](+++) high expression; (+) low expression; (−) not expressed.

morpholino-oligonucleotides (*ap1m1*MO, *ap1m2*MO, and *ap1m3*MO). *ap1m1*MO and *ap1m3*MO interfered with the splicing of the 3′-end of exon 5 while *ap1m2*MO interfered with splicing of the 3′-end of exon 3. In all cases, the splicing-inhibiting morpholinos (MOs) were predicted to yield truncated, nonfunctional proteins. RT-PCR analysis of these morphants at 24 and 48 hpf confirmed the targeting efficacy of the three MOs (data not shown). The vast majority of *ap1m1*MO morphants (97% n = 66/70) exhibited head malformation at 24 hpf and a severe phenotype of the central nervous system. Morphants showed poorly defined midbrain–hindbrain boundaries in the cerebellum region compared with controls (Fig. 5A:a–f). The defects became even more pronounced at 48 hpf (Fig. 5B:c,d). No anomalies have been observed in the vascular and the cardiac apparatus. Zebrafish μ1A-deficiency causes developmental defects comparable with μ1A-deficiency in mice (Meyer et al., 2000), despite the presence of μ1C in zebrafish CNS. A significant percentage of *ap1m3*MO morphants (n = 80; 95%), similarly to *ap1m1*MO morphants showed a severe phenotype in main nervous structures (cerebellum, midbrain, hindbrain, and midbrain–hindbrain boundary). Additionally we could observe an alteration in the structure of somites (Fig. 5A:g–i). At 48 hpf the phenotype of *ap1m3*MO morphants (93%) is still similar to *ap1m1*MO morphants, but in addition, we observed a severe alteration in the forebrain ventricle in comparison to control and *ap1m1*MO morphants. Somites are poorly defined and the morphants exhibited a mild edema (Fig. 5B:a,e). Both *ap1m1*MO and *ap1m3*MO embryos showed severe

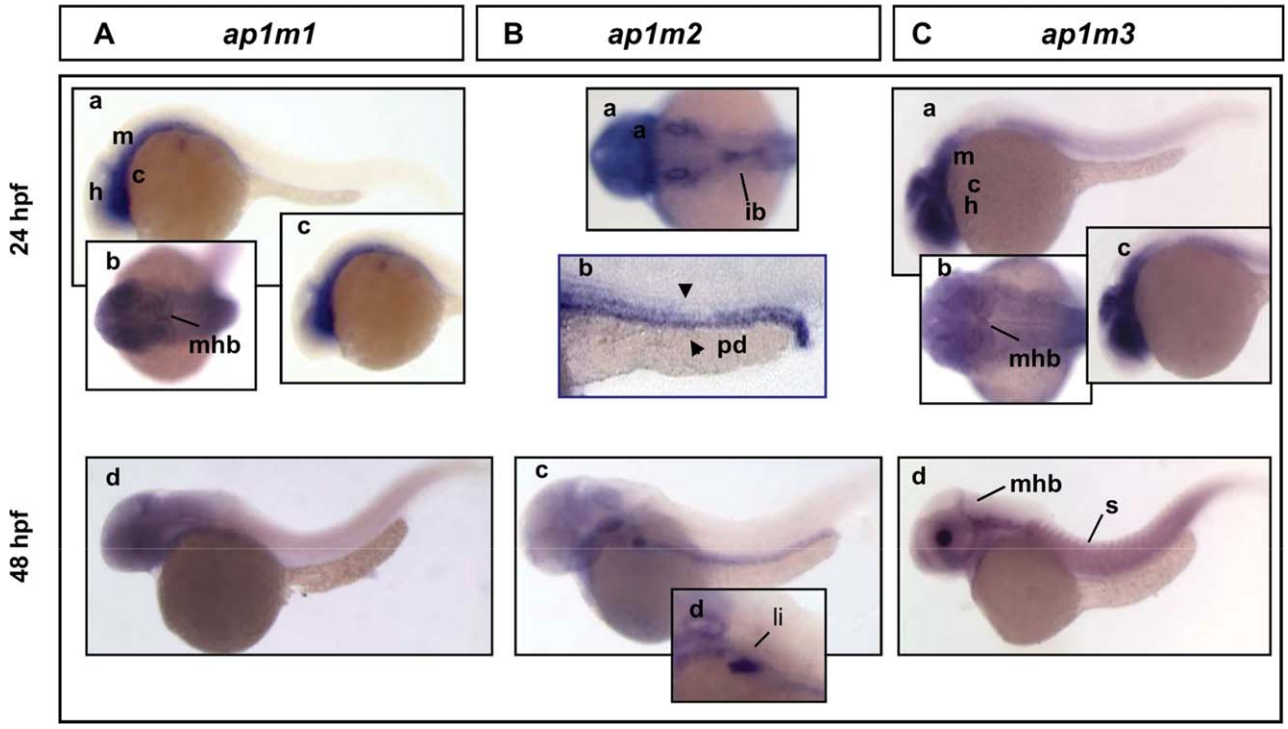

Fig. 4. Expression analysis of zebrafish μ1 adaptins by WISH at 24 and 48 hpf. **A:** *ap1m1* is expressed in defined brain regions at 24 hpf (a,b c) and 48 hpf (d). a,c,d: lateral view anterior to the left. b: dorsal view **B:** (a–d) *ap1m2* transcript is expressed in intestinal bulb (a) and pronhephric ducts at 24 hpf (b). At 48 hpf the transcript expression is still detectable in the digestive tract (c) and liver (d). b,c,d lateral view anterior to the left; a: dorsal view. **C:** (a–d) The *ap1m3* transcript is detectable at 24 (a,b,c) and 48 hpf (d). Expression in different CNS structures: midbrain, hindbrain and cerebellum (a) and midbrain–hindbrain boundary (d). At 48 hpf a label of *ap1m3* is detectable in somites (d). m, midbrain; h, hindbrain; mhb, midbrain–hindbrain boundary; c, cerebellum; s, somites; pd, pronephric duct; ib, intestinal bulb; li, liver.

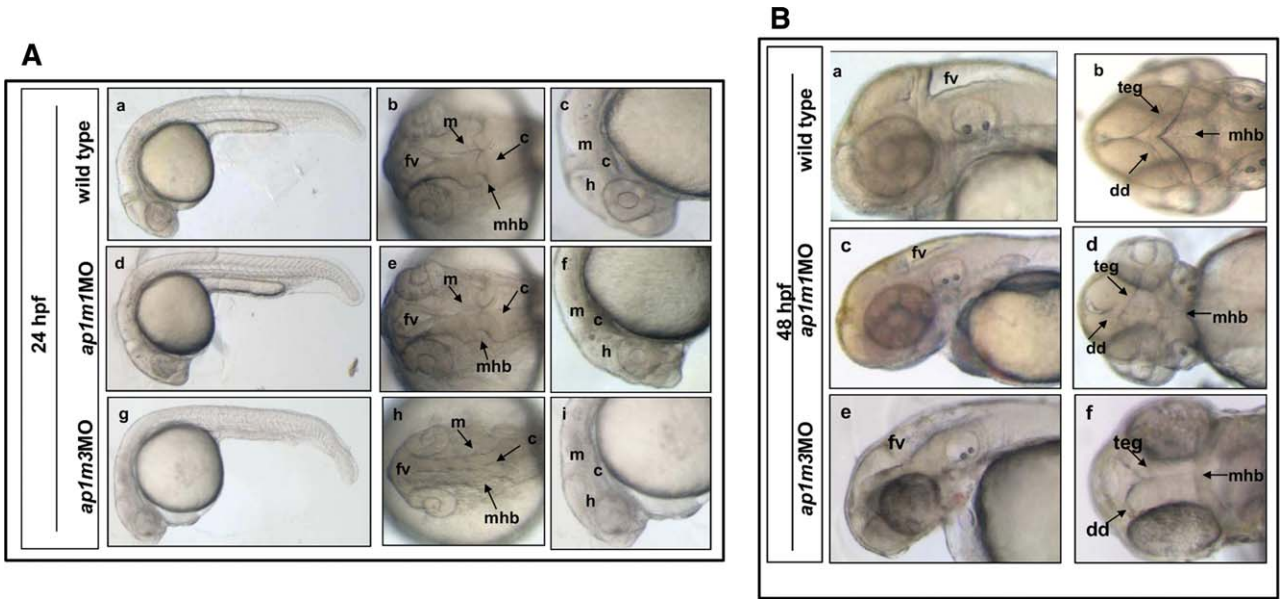

Fig. 5. Morphological defects in *ap1m1*MO and *ap1m3*MO single morphants. Embryos were injected at the two-cell stage and examined at 24 and 48 hpf. **A:** Lateral view and dorsal view at 24 hpf. Single morphants of *ap1m1* and *ap1m3* exhibit brain malformations (d,e,g,h) with unclear boundaries between brain subdivisions, especially at hindbrain and midbrain region (f,i). *ap1m3*MO morphants showed poorly defined somites (g). **B:** At 48 hpf, CNS abnormalities became more pronounced. The forebrain ventricle in both single morphants (c,e; control in a). Dorsal view of *ap1m1*MO and *ap1m3*MO embryos revealed a severe disorganization of CNS structures (d,f). a,c,e: lateral view anterior to the left. b,d,f: dorsal view. h, hindbrain; c, cerebellum; teg, tegmentum; dd, dorsal diencephalon; mhb, midbrain–hindbrain boundary; m, midbrain; fv, forebrain ventricle.

mobility defects and delay in "hatching" from *chorion*. The *ap1m2*MO morphants confirmed the published data with defects in gut, kidney and liver development (Zizioli et al., 2010), with no evident alterations in brain regions. The major effects observed in single morphants are summarized in Table 4. Because of the described partial suppression of μ1-deficiencies by isoforms in mouse, we also performed double-knockdown experiments of *ap1m1* (μ1A) and *ap1m2* (μ1B), the two zebrafish orthologs of the mammalian adaptins. Co-injection of *ap1m1* and *ap1m2* morpholinos (*ap1m1*MO/*ap1m2*MO) enhanced the alterations induced by single morpholino. At 24 hpf the central nervous system is more severely affected, despite a hardly detectable

TABLE 4. Summary of Morphant Phenotypes[a]

24 hpf				
MORPHOLOGICAL DEFECTS	*ap1m1MO*	*ap1m2*MO	*ap1m1*/*ap1m2*MO	*ap1m3*MO
Brain	+++	n.d	++	+++
Poorly defined somites	n.d	n.d.	n.d	+++
Gut	n.d.	+	+	n.d
Kidney	n.d.	+++	++	n.d
Cardiovascular system	n.d.	n.d	n.d	n.d

48 hpf				
MORPHOLOGICAL DEFECTS	*ap1m1MO*	*ap1m2MO*	*ap1m1*/*ap1m2*MO	*ap1m3*MO
Brain	+++	n.d	++	+++
Poorly defined somites	n.d	n.d	+	+++
Gut	n.d	++	+	n.d
Kidney	n.d.	+++	+++	n.d.
Presence of edema	n.d.	+	+++	++
Cardiovascular system	n.d.	n.d	n.d	n.d
Hatching	+	+	+	++

[a]+++ (strong alteration); ++ (medium alteration); + (mild alteration); n.d: not detected.

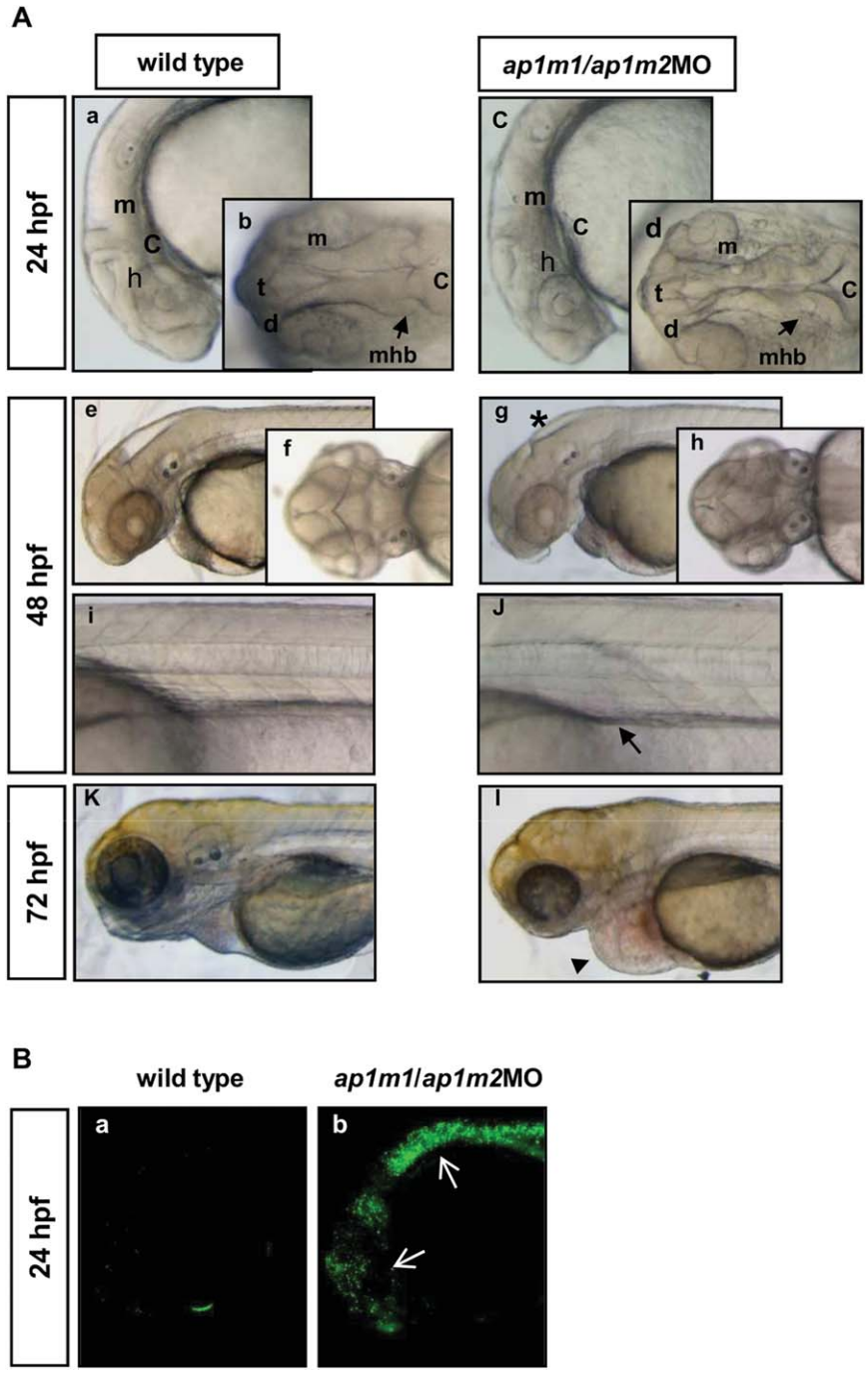

Fig. 6. Morphological defects and apoptosis in *ap1m1/ap1m2*MO double morphants. **A:** Two-cell stage embryos were injected with 0,6 pmol/embryo of *ap1m1*MO plus 0,4 pmol/embryo of *ap1m2*MO. At 24 hpf, double morphants (c; control a) showed brain malformations with a disorganization of the midbrain–hindbrain boundary. At 48 hpf, the ventricular cavity is reduced (g,h; forebrain ventricle: black asterisk). The proximal tubule appeared irregular and not clearly defined than in wild-type embryos (i, j arrow). At 72 hpf, in double morphants the edema (arrowhead) is more pronounced (controls k,l). a, c, e, g, i, j, k, l: lateral view, anterior to the left; b,d,f,h: dorsal view. m, midbrain.; t, telencephalon; d, diencephalons; mhb, midbrain–hindbrain boundary; c, cerebellum. **B:** Wild-type (a) and *ap1m1/ap1m2*MO (b) were incubated at 24 hpf with acridine orange (AO) and then analyzed by laser confocal microscopy. Apoptotic cells are detected in the CNS of double morphants.

μ1B (Ap1m2) expression (Fig. 6). Telencephalon, diencephalon, and midbrain are compromised and the hindbrain–midbrain boundary is not well defined compared with wild-type embryos (Fig. 6A:a–d). The phenotype was more pronounced at 48 hpf (Fig. 6A:e–h). In comparison with control embryos, we observed a reduction of ventricle size in double knockdown embryos (Fig. 6A:e,g) and the brain structures (hindbrain, midbrain, and midbrain–hindbrain boundary) appear more compromised than at 24 hpf (Fig. 6A:f,h). At this developmental stage in vivo analysis reveals that in double morphants the proximal region of pronephric ducts is more irregular

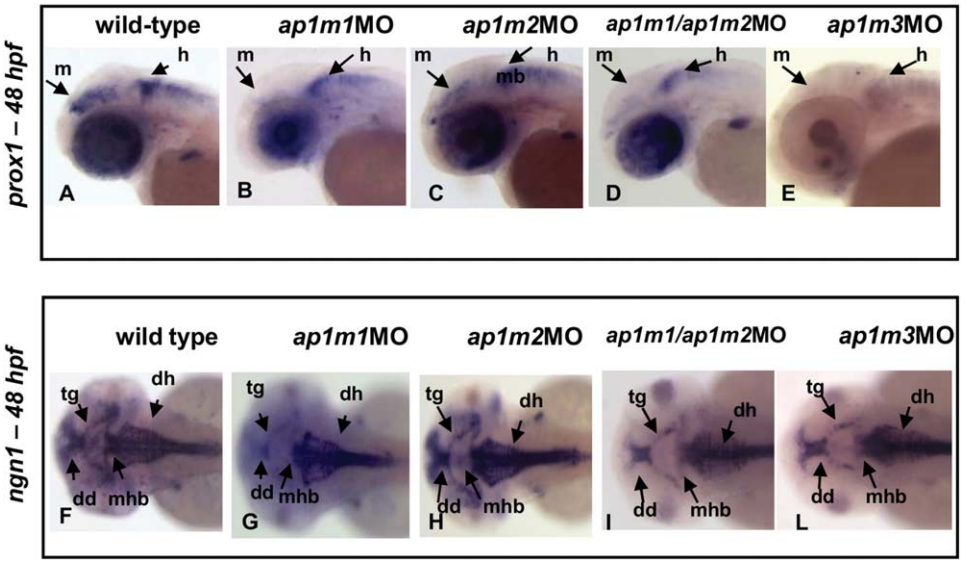

Fig. 7. Single and double *ap1m1/ap1m2*MO knock-down affects CNS development. At 48 hpf, the expression of the neural markers *prox1* and *ngn1* were investigated by WISH in single and double morphants. Wild-type (A,F), single and double morphants (B–E,G–L). Lateral (A–E) and dorsal view (F–L) are shown. Altered expression of both markers is affected in several regions of the CNS. Abbreviations: m, midbrain; h, hindbrain; tg, tegmentum, dh, dorsal hindbrain; dd, dorsal diencephalon, mhb, midbrain–hindbrain boundary.

and less defined than in control embryos (Fig. 6A:i,j). At 72 hpf, in addition to morphological defects in CNS and in pronephric ducts, we observed cardiac edema (Fig. 6A:k,l). The presence of edema indicates loss of renal function and abnormal formation of pronephric ducts. Thus Ap1m1/Ap1m2 (μ1A/μ1B) deficiency during kidney development enhances the phenotype of Ap1m2 (μ1B)-deficiency, whereas Ap1m1 (μ1A)-deficiency alone only moderately impairs gut and kidney development. Moreover, despite its hardly detectable expression in CNS, μ1B appears to play a significant role in brain development. To assess whether apoptotic events occur in μ1A/μ1B double-deficient embryos, we used the acridine orange test to label apoptotic cells (Cole and Ross, 2001). Confocal analysis, performed at 24 hpf, clearly demonstrates a significant increase in the number of apoptotic cells throughout the developing brain of double morphants (Fig. 6B:a,b). Double morphants also showed reduced hatching from the *chorion* and they showed a delay "*in response to touch*" (Unpublished observations G. Gariano and D. Zizioli). In Table 4, we summarized all the defects of single and double morphants. The similarities and differences in expression of *ap1m1* and *ap1m3* suggest, that they may be functionally redundant in domains, where both are expressed such as developing midbrain, hindbrain and midbrain–hindbrain boundary, but that they also might have specific functions in other domains. Together these data suggest that both, μ1A and μ1B, have different and specific roles in CNS development and kidney formation and that μ1C cannot compensate for the loss of either isoform.

Expression Markers for Brain and Kidney Development in Single and Double-Knockdown Experiments

We used molecular markers to study the early events of CNS development and pronephric duct formation following the single (*ap1m1*, *ap1m2*, and *ap1m3*) and simultaneous knockdown of μ1 encoding genes. We analyzed the expression pattern of the basic helix-loop-helix transcription factors *neurogenin-related gene-1* (*ngn1*), the paired-box transcription factor *pax2.1* and the homeobox gene *prox1*. *ngn1* is specifically expressed during CNS development in zebrafish, being detectable 2 hr before the more restricted *nrd* expression (Mueller and Wullimann, 2002; Li et al., 2010). At the end of gastrulation *ngn1* expression is initiated in the neural plate; at later stages its expression is detectable in the tegmentum, dorsal diencephalon, posterior midbrain, midbrain boundary, hindbrain area, optic stalk, and spinal cord (Korzh et al., 1998). *prox1* is widely expressed in several districts of the central nervous system (Pistocchi et al., 2008). Specifically, *prox1* was found to be expressed in a group of neurons located in the pretectal segment (that belongs to midbrain region), as well as segmentally arranged cells of hindbrain (Liu and Joyner, 2001). *pax2.1* has been shown to be an essential regulator of nephrogenesis in higher vertebrates (Torres et al., 1995). At early stages of development, *pax2.1* is expressed by the intermediate mesoderm (Puschel et al., 1992). Additionally, several studies have defined that at early stages of nephron morphogenesis (24–30 hpf), *pax2.1* labels proneprithic ducts, the earliest epithelial structure derived from intermediate mesoderm. In zebrafish, the no isthmus mutation (*noi*) revealed the importance for *pax2.1* expression for the maintenance of the pronephric duct epithelia. Generation of epithelial cell polarity is the result of a process guided both by environmental signals and by spatial cues intrinsic to the cell. The multiple steps involved in the initiation and

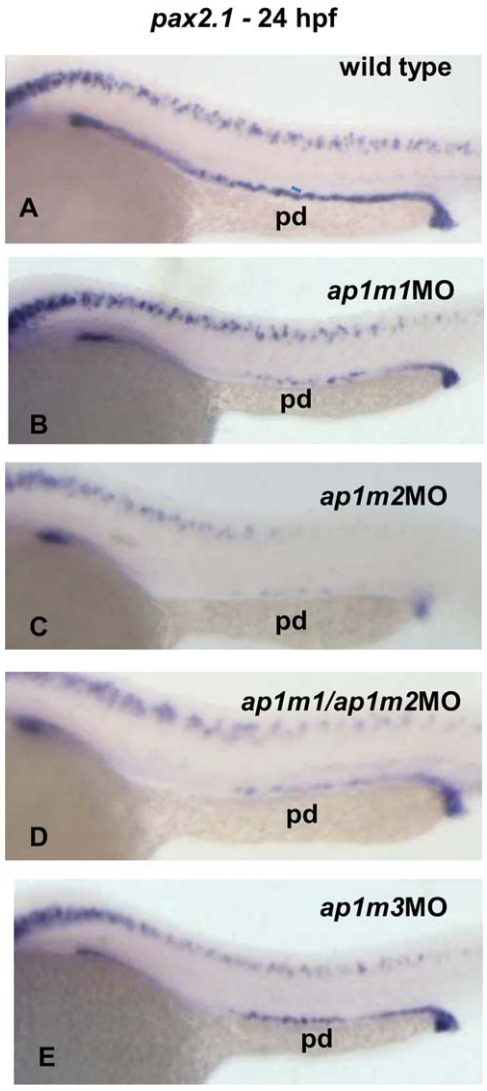

Fig. 8. **A–E**: Effects of μ1 knockdowns on *pax2.1* expression. At 24 hpf, wild-type embryos, single and double morphants were analyzed by WISH for *pax2.1* expression. Expression of *pax2.1* is down regulated in *ap1m2*MO and in double morphants *ap1m1/ap1m2*MO (C,D; control A). *pax2.1* expression is not affected in single *ap1m1*MO and *ap1m3*MO morphants (B,E). pd, pronephritic duct; (A–D) lateral views anterior to the left.

maintenance of membrane asymmetry include intracellular vesicular targeting by adaptor complexes (Dressler and Woolf, 1999; Majumdar et al., 2000; Serluca and Fishman, 2001). First, we analyzed the expression of *prox1* and *ngn1* at 48 hpf, in single and double *ap1m1*/*ap1m2*MO morphants, respectively. A reduced expression of both *prox1* and *ngn1* genes and disorganization of different CNS areas was detectable by WISH analysis in all cases studied. In particular, a significant reduction of *prox1* expression was detected in the midbrain region, dorsal diencephalon and telencephalon in single (*ap1m1*MO; *ap1m3*MO) and double morphants (Fig. 7B,D,E) in comparison to controls (Fig. 7A). The reduction in *prox1* expression was not dramatic in the *ap1m2*MO, where a faint labeling of these structures is still present (Fig. 7C). Also, a subtle reduction and/or partial disorganization of *ngn1* expression was detected in anterior brain areas (including tegmentum, dorsal diencephalon, and midbrain–hindbrain boundary). The observed phenotype was more severe in single *ap1m1*MO, *ap1m3*MO and *ap1m1*/*ap1m2*MO double knockdown embryos (Fig. 7G,I,L) compared with *ap1m2*MO single morphants and controls (Fig. 7F,H). We next analyzed *pax2.1* expression at 24 hpf (Fig. 8) and noticed major alterations in kidney formation. The pronephric duct forms primarily through the recruitment of intermediate mesoderm at all axial levels followed by in situ polarized epithelial cells, a central process in kidney formation in all vertebrates (Drummond et al., 1998). By the end of this transition, epithelial cells are polarized with an apical brush border and a basolateral membrane domain containing ion transport proteins that are essential for the osmoregulatory function of the duct. At 24 hpf *pax2.1* down-regulation was observed in the mesoderm primordium in single *ap1m2*MO and double morphants (data not shown). A strong down-regulation of *pax2.1* was revealed at the level of proximal tubule in *ap1m2*MO single and partially in *ap1m1*/*ap1m2*MO double morphants (Fig. 8C,D). In contrast, *ap1m1*MO and *ap1m3*MO single morphants were unaffected (Fig. 8B,E). These data indicate that kidney formation specifically depends on μ1B. To assess this hypothesis, we examined cross-sections of 2-days embryos embedded in paraffin. We analyzed glomerulus, pronephric ducts, liver and gut in uninjected embryos (Fig. 9A,B,E) and in *ap1m1*/*ap1m2*MO morphants (Fig. 9C,D,F). The morphant embryos showed an irregular pronephric ducts development, with a thinner and disorganized pronephric epithelium and irregular lumen (Fig. 9C,D) compared with controls (Fig. 9A,B). These data suggest that knock-down of the μ1B (Ap1m2) alters the overall development of polarized tissue. We found that double morphants showed hepatic hypertrophy with high hypercellularity. The increased liver volume collapses the gut lumen (Fig. 9E,F). Furthermore, μ1B could be involved in muscle morphogenesis, because the myotome boundaries and nuclei alignment were not clearly delimited (Fig. 9E,F). The latter finding could be related to the mobility defects.

Ap1m2 (μ1B) Adaptin Function in Kidney Development

To investigate whether, besides a structural and morphological kidney

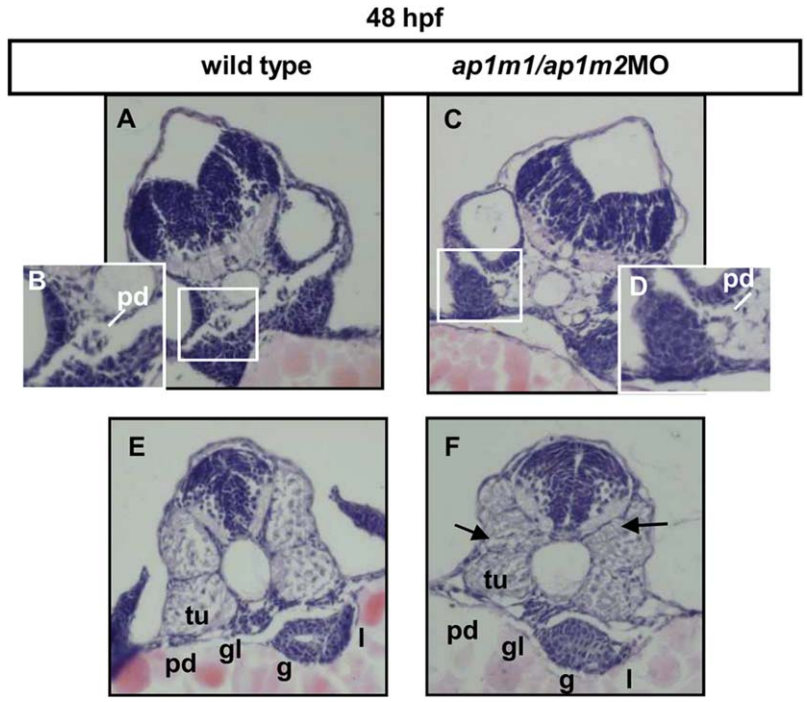

Fig. 9. **A–F**: Histological analysis of double morphants. At 48 hpf zebrafish *ap1m1/ap1m2*MO double knockdown embryos were embedded in paraffin and sectioned at trunk level (H&E staining). Transverse sections (7μm) revealed disturbed pronephritic duct development (C,D; controls A,B); (see boxed areas in panel A and C). Structures in the anterior part as pronephric ducts, gut, liver in control (E) and double morphants (F). In double morphants the lumen of gut and the cell polarity are lost, liver morphology is severely compromised, the pronephric ducts are not well formed (F). An altered myotome organization is also detected (F, black arrows; control E). Abbreviations: pd, pronephric duct; g, gut; tu, tubule; gl, glomerule; l, liver.

rearrangement, Ap1m2 (μ1B) knockdown may influence also the correct kidney functions, we performed mannitol treatment and dye filtration experiments. The primary function of zebrafish kidney is osmoregulation, and larvae with kidney functional impairment develop severe edema. Edema results from decreased water export and can be interpreted as a malfunction of the renal and circulatory system (Hill et al., 2004). Treatment with 250 mM mannitol causes significant reduction of pericardial edema. At 72 hpf, in vivo experiments have shown that the vast majority of double *ap1m1/ap1m2* morphants (95%) exhibited a severe edema. We decided to treat the double morphants (n = 40) with mannitol and followed their development over 1, 2, and 3 days after the treatment (Fig. 10A). After 1 day, 97% of the treated embryos showed a reduction of edema in comparison to untreated embryos (Fig. 10B,C). The complete reabsorption of the edema was achieved after 2 and 3 days of treatment in 95% of embryos (Fig. 10D,F). In untreated embryos (n = 40), the edema became more pronounced all over the yolk sack after 2 or 3 days in 95% of the animals (Fig. 10E,G).

Glomerular filtration is an essential element of renal function, generating the blood filtrate which is then selectively modified by transport processes in the renal tubules (Drummond et al., 1998). To determine, whether kidney filtration is compromized in *ap1m1/ap1m2* morphants, rhodamine dextran (10,000 *M*r) was introduced into the circulatory system both in wild-type and morphants embryos by sinus venosus injection at 48 hpf (Fig. 11A,B). Images were obtained at days 1, 2, and 3 postinjection (dpi). If the kidney is functionally active, dextran is expected to pass through the glomerular basement and the pronephric ducts, and should be secreted (Kramer-Zucker et al., 2005). Initially fluorescent dextran was trapped in the yolk at the site of injection close to the heart, both in controls and in morphants (Fig. 11A,B). Already at 1 day postinjection, the fluorescent dextran was significantly reduced in control larvae, while in *ap1m1/ap1m2* morphants a significant fluorescent signal was detected (Fig. 11C,D). The fluorescent signal was still visible even after 3 and 4 dpi in morphant embryos and was spread out (Fig. 11E–H).

DISCUSSION

We describe here the analysis of the three μ1-adaptins A, B, and C, encoded in the zebrafish genome extending our previous analysis on μ1-adaptin functions in this model organism (Zizioli et al., 2010). Mammals express only the two μ1-adaptins: μ1A and μ1B, which have been characterized in detail. In the mouse, μ1A is expressed in all adult tissues, with a pronounced increase in brain, whereas μ1B expression is restricted to polarized epithelia (Boehm and Bonifacino, 2002; Robinson, 2004). In mice, μ1A-deficiency is lethal at midorganogenesis (13.5 d), while μ1B-deficient mice are viable and fertile (Meyer et al., 2000; Takahashi et al., 2011; Hase et al., 2013).γ1-deficiency in mice, which corresponds to a μ1A/μ1B-double deficiency, leads to the arrest of development already at the blastocyst stage, indicating that μ1A-deficient mice develop further, because of the presence of the polarized epithelia specific μ1B (Zizioli et al., 2010). It was shown that μ1A and μ1B can indeed partially compensate each other in protein sorting, presumably in "house-keeping" functions (Eskelinen et al., 2002; Gonzalez and Rodriguez-Boulan, 2009; Gravotta et al., 2012). AP-1A and AP-1B specific protein sorting functions are in part mediated by their specific targeting to different organelles, AP-1A predominantly to the TGN and early endosomes and AP-1B to basolateral recycling endosomes (Folsch et al., 2001; Krauss et al., 2006; Fields et al., 2010). In addition μ1A, and possibly μ1B, plays a role in the regulation of AP-1A membrane-cytoplasma recycling, which is essential for proper protein sorting (Medigeshi et al., 2008; Radhakrishnan et al., 2013).

The dependence of zebrafish development on AP-1 mediated protein sorting pathways appears to be more

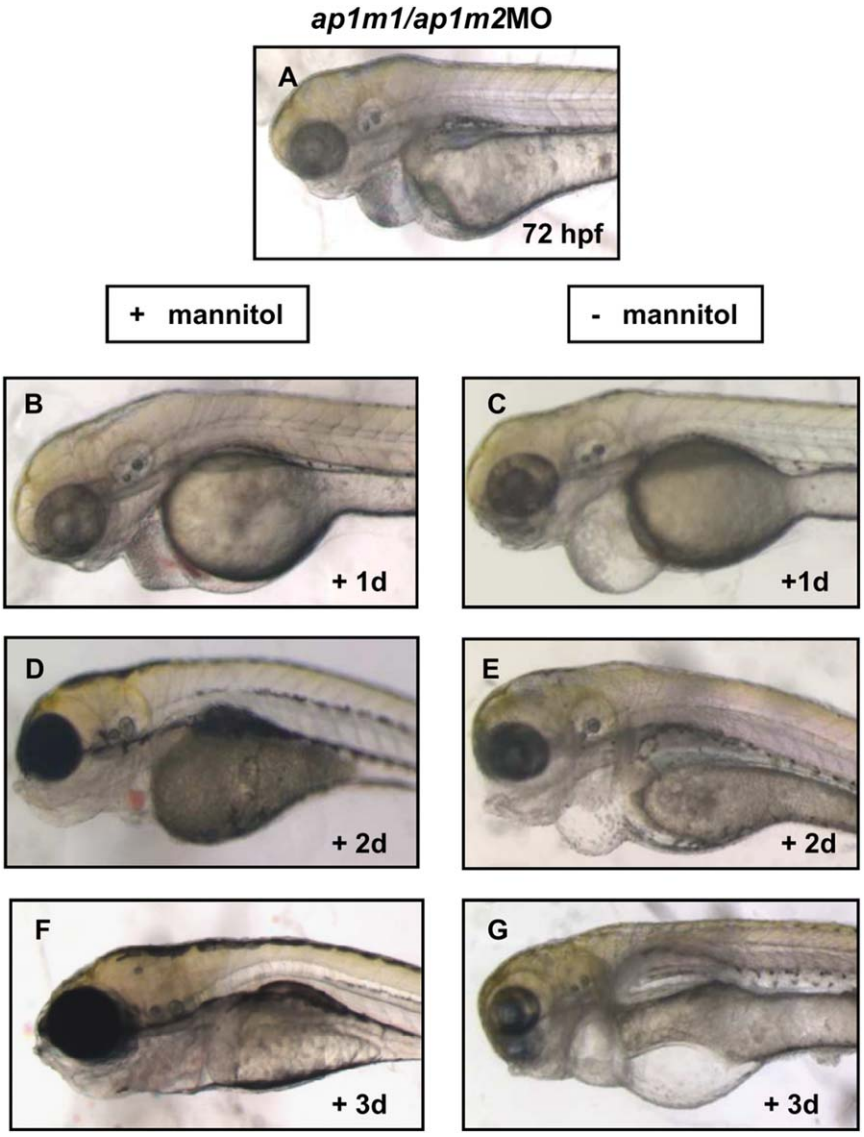

Fig. 10. **A–G**: Mannitol treatment of edema. Double morphants with severe edema at 72 hpf (A), were exposed to 250 mM mannitol for 1, 2, and 3 days. After day 1 treated embryos showed a strong reduction of edema (B), which improved further (D,F; controls C,E,G).

complex because zebrafish has three μ1-adaptins. In a previous study we have shown that μ1B is expressed in zebrafish liver, in contrast to mouse embryonic and adult liver, and that its deficiency indeed impairs liver development (Zizioli et al., 2010). Here we show that despite the fact that liver development appears to be unaffected in μ1A-deficient zebrafish and mice, the zebrafish phenotype is enhanced by μ1A/μ1B double-deficiency. This indicates also μ1A specific functions in liver development, which were not apparent in mice up till day 13.5 (Meyer et al., 2000). This demonstrates organism specific mechanisms in liver development, which are currently not understood.

μ1B-deficiency and μ1A/μ1B double-deficiency severely affect pronephritic ducts, kidney development and function in zebrafish, in line with essential μ1B functions in basolateral protein sorting. However, such a phenotype has not been reported for μ1B-deficient mice, despite high μ1B expression in embryonic and adult kidney (Ohno et al., 1999; Takahashi et al., 2011; Hase et al., 2013).

Despite its high expression in mouse kidney, m1B is not expressed in all cell types. Proximal tubule cells do not express it and consequently some proteins, which are sorted basolateral by AP-1B in other cells, are found at the apical site in proximal tubule cells, although these cells do express AP-1A (Schreiner et al., 2010). This cell-type specific expression raises the question, whether all kidney cells express AP-1B during development and that its expression is selectively down regulated later or whether it is not expressed during early stages of development and then expressed in a subset of cells. The zebrafish phenotype demonstrates AP-1B functions already at early stages of development. It is presently unknown in which way zebrafish kidney development depends on AP-1B, but mouse kidney development does not, indicating that in the absence of AP-1B mouse cells have alternative mechanisms for effective basolateral sorting assuring proper tissue morphology (Perez Bay et al., 2013).

μ1A-deficiency in zebrafish causes severe defects in CNS development, comparable to those observed in μ1A-deficient mice, which do not express a μ1C isoform. These embryos have severe hemorrhages in the ventricles and the spinal canal, which were detected already at day 7.5 (Meyer et al., 2000). In AP-1A "knock-down" primary neuron cultures, AP-1A dependent basolateral/dendritic sorting was demonstrated as in other polarized cell lines (Farias et al., 2012). However, the AP-1A/σ1B complex is also required for the apical presynaptic recycling of synaptic vesicles and this form of cell–cell communication (Glyvuk et al., 2010). The μ1C expression pattern largely mirrors that of μ1A and because of their high sequence homology, μ1C could just be an isoform without any specific function. The fact that μ1A/μ1B double-deficient zebrafish develops until organogenesis, whereas γ1-deficiency in mice (corresponds to a μ1A/μ1B double-deficiency) leads to developmental arrest at the blastocyst stage, indicates that zebrafish μ1C expression levels are high enough to sustain major AP-1 dependent protein sorting functions (Zizioli et al., 1999). Moreover, despite a hardly detectable μ1B expression in zebrafish CNS, it also appears to fulfil specific functions in brain development as indicated by the

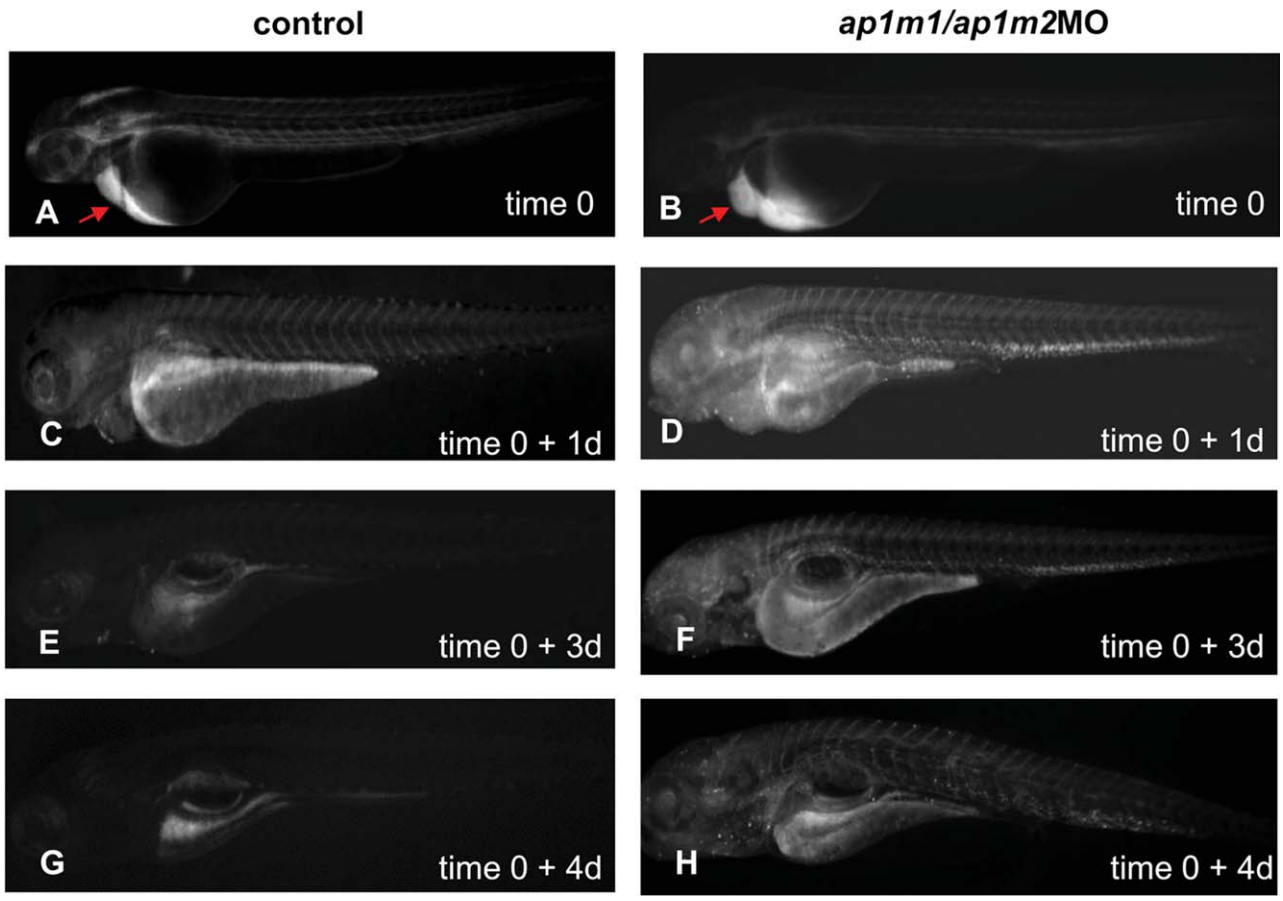

Fig. 11. A–H: Impairment of glomerular filtration in *ap1m1/ap1m2*MO morphants. Control embryos (A,C,E,G) and *ap1m1/ap1m2* morphants (B,D,F,H) were injected with rhodamine dextran (10.000 Mr) in the sinus venosus at 48 hpf. The dye was readily removed in control embryos (C,E,G), but it was still present in morphants even after day 4 (D,F,H).

more severe phenotypes of μ1A/μ1B double-deficient animals. However, it is not clear whether this is due to defects in neuroblasts or in neighboring polarized epithelia. Besides μ1A (AP-1A) also μ1C (AP-1C) has specific functions in zebrafish CNS development as they cannot compensate for each other. In addition, μ1C plays a role in somite formation and its reduced expression causes edema, without apparent defects in pronephric duct development.

The demonstrated specific functions of μ1 isoforms in tissue development raises the question about the molecular mechanisms by which an isoform fulfils its function. Three μ1-adaptin functions have been identified so far: binding of a subset of AP-1 cargo proteins, targeting of AP-1 complexes to specific organelles (μ1B), regulation of AP-1 complex membrane-cytoplasm recycling (μ1A) (Bonifacino and Traub, 2003; Medigeshi et al., 2008; Fields et al., 2010; Radhakrishnan et al., 2013). Comparing the structures of the three zebrafish μ1-adaptins reveals a clustering of specific residues at the μ1-β1 interface. The interaction of the μ-adaptin N-terminal globular domains with the corresponding β-adaptin is required for hemi-complex formation and thus AP-complex assembly, whereas the interaction of the C-terminal μ-adaptin domains with β-adaptins is less stable and has to be released, because the β-adaptin covers up the μ-adaptin cargo binding domain (Collins et al., 2002; Heldwein et al., 2004; Jackson et al., 2010). The conformational change of the μ-adaptins is supported by its phosphorylation in the flexible domain between the two N- and C-terminal domains (Conner et al., 2002; Ricotta et al., 2002; Ghosh et al., 2003). Alterations of the μ-β interface could change the way this opening of the AP-complex is regulated. This would allow to individually regulate μ1-isoform protein sorting activities by selective targeting of the respective AP-1 complex to a specific organelle. A detailed electron microscopic analysis of the subcellular localization of the AP-1 complexes would be a first step to test this model. The differences between mouse and zebrafish in the dependence of liver and kidney development on μ1A and μ1B, and the existence of μ1C only in zebrafish point to important differences in AP-1A, AP-1B, and AP-1C dependent protein sorting pathways essential for tissue development in mouse and zebrafish. It is essential to understand these differences in the developmental pathways. Comparison of μ1 structures point to domains, which might be essential for isoform specific functions and thus the regulation of their specific functions in vertebrate development.

Developmental Dynamics

EXPERIMENTAL PROCEDURES

Ethics Statement

All embryos were handled according to relevant national and international guidelines.

Fish and Embryos Maintenance

Adult zebrafish of the wild-type AB line were raised and maintained at 28°C on a 14/10 hr light/dark cycle according to established techniques (Westerfield, 2007). Embryos were collected by natural spawning and staged according to (Kimmel et al., 1995). Embryos for WISH were raised, from 18-hpf throughout development, in 0.003% 1-phenyl-2-thiourea (Sigma) to prevent pigmentation and fixed in 4% paraformaldehyde (PFA).

Gene Identification and Sequence Analysis

The mouse amino acid reference sequences of Ap1m1 (access no. NP_031482) and Ap1m2 (access no. NP_033808.2) were used as a query in a series of Blast searches versus nucleotide and polypeptide zebrafish sequences present in NCBI databases. This analysis led to identification of two putative zebrafish orthologs: *ap1m1* (access no. XM_002660720) and *ap1m2* (access no. NM_205714). More recently, we identified a novel sequence (access no. NM_001114441) belonging to a third gene that, following the advice of the Zebrafish Nomenclature Committee (http://zfin.org/zf_info/nomen.html) we have named *ap1m3*.

A multiple sequence alignment (MSA) was generated using the ClustalW algorithm (Thompson et al., 1994) starting from Ap1m1 (*Danio rerio* access no. XP_002660766), (*Homo sapiens* access no. NP_115882.1), (*Mus musculus* access no. NP_031482) and (*X. tropicalis* access no. NP_989033); Ap1m2 (*Danio rerio* access no. NP_991277), (*Homo sapiens* access no. NP_005489.2), *Mus musculus* (access no. NP_033808), and *X. tropicalis* (access no. NP_001006851.1) and Ap1m3 (*Danio rerio* access no. NP_001107913.1) amino acids sequences. From the alignment, a bootstrap phylogenetic tree was generated using the neighbor-joining algorithm (Guindon and Gascuel, 2003; Edgar, 2004). For the generation of the tree, a MSA was generated including also the sequence of the Ap1m1 polypeptide from *Caenorhabditis elegans* (encoding the μ1 subunit of the AP-1 complex in the worm access no. NP_491572.2) that has been used as outgroup sequence.

RNA Isolation and RT-PCR

Total RNA was isolated from 30 embryos at multiple stages of development and from different adult organs and tissues (ovary, muscle, brain, kidney, liver, and gut) using TRIZOL reagent (Invitrogen, Carlsbad, CA) according to manufacturer's protocol. Gene-specific primers used as indicated below.

ap1m1: Forward 5′-gcagcatgggatccacaaattcaggt-3′; Reverse 5′-ccttagcaatctaagaatgcgcacct-3′

(Tm = 60°C 35 cycles - product size: 1,200 bp)

ap1m2: Forward 5′-ggaatgtgacttaactctgctttagcc-3′; Reverse 5′-cgattattacagcattaggagaaaca-3′

(Tm = 60°C 35 cycles - product size: 1,600 bp)

ap1m3: Forward 5′-tgccaataatgtgtccatcttag-3′; Reverse 5′-ctcttgccctccagttcatcac-3′

(Tm = 55°C 35 cycles - product size: 204 bp)

Zebrafish α-Elongation Factor 1 (EF-1α) was used as loading control, using specific primers

(For 5′-GGTACTTCTCAGGCTGACTGT-3′; Rev 5′-CAGACTTGACCTCAGTGGTTA-3′) as described (Gilardelli et al., 2004).

WISH

WISH were carried out essentially as described by (Thisse and Thisse, 2008). The probes specific for each gene were designed on coding sequences to avoid cross-hybridization among the different genes as indicated below:

ap1m1: Forward 5′-gtccgttaacctcctggtcagtg-3′; Reverse 5′-ccatgaatgcgagctgtagcc-3′

(Tm = 54°C 33 cycles - product size: 831 bp)

ap1m2: Forward 5′-ccgctaaacaccggaatgtgactttac-3′; Reverse 5′-cccgacagcatcgtcttcagtctgatg-3′

(Tm = 60°C 35 cycles - product size: 701 bp)

ap1m3: Forward 5′-tgaaagcagaaagattacatacga-3′; Reverse 5′-ttgagcacaaaatgttgtcaat-3′

(Tm = 55°C 35 cycles - product size: 960 bp)

The templates for the digoxigenin (DIG) -labeled probes were the following: nucleotides 721–1549 of *ap1m1* (access no. XM_695500), nucleotides 64–765 of *ap1m2* (access no. NM_205714), and 3499–4465 of *ap1m3* (access no. NM_001114441) subcloned into pGem-T Easy vector (Promega). All constructs were verified by sequencing. The antisense and sense control probes were produced with SP6 and T7 RNA polymerases (Roche) after linearization with *Not*I for *ap1m1*, *Sac*I for *ap1m2*, and *Spe*I for *ap1m3* in the presence of DIG-labeled nucleotides (Roche). Whole-mount images were taken with a Leica MZ16F stereomicroscope equipped with DFC 480 digital camera and LAS Leica Imaging software (Leica, Wetzlar, Germany). Magnification ×50, ×63, and ×80.

Morpholino Injections

Antisense morpholino oligonucleotides *ap1m1*MO, *ap1m2*MO and *ap1m3*MO were purchased from Gene Tools (Philomat, OR) and designed to interfere with the normal RNA splicing of *ap1m1*, *ap1m2*, and *ap1m3* mRNAs, respectively. *ap1m1*MO (5′-GTATCTGTGTATCGACACACAATGA-3′) was designed to anneal to the intron 4-exon 5 boundary of *ap1m1*, *ap1m2*MO (5′-GCTCGGTCAGTCTGGGGTGTGTGTGTGTGT-3′) annealed to the exon 3-intron 3 boundary of *ap1m2* whereas *ap1m3* (5′-CTGAGTAATATACCTGGTGTGGAAA-3′) annealed to the intron 4-exon 5 boundary of *ap1m3*. Two additional morpholino oligonucleotide was designed to target each gene: an additional splice-site morpholino for *ap1m1* and a morpholino targeting the translational starting site for *ap1m2*. These morpholinos confirmed *ap1m1*MO and *ap1m2*MO phenotypic effects. Escalating doses of single (from 0.5 pmol/embryo to 1.5 pmol/embryo) and double MOs were

tested for phenotypic effects and we established an optimum concentration at 0.8 pmol/embryo for single injections of *ap1m1*MO, 0.5 pmol/embryo for single injections of *ap1m2*MO and 1 pmol/embryo for single injection of *ap1m3*MO; co-injection experiments were performed at 0.6 pmol/embryo *ap1m1*MO and 0.4 pmol/embryo *ap1m2*MO). The morpholinos were diluted either alone or simultaneously with 1× Danieau buffer and injected into one-to four-cells stage embryos. After microinjection, embryos were incubated in egg water supplemented with 0.003% PTU at 28°C to prevent pigmentation process. Embryos development was valued at 24 hpf, 48 hpf, and 72 hpf.

Histologic Analysis

After morpholino injection, embryos at 24 hpf and 48 hpf were fixed in 4% PFA, paraffin-embedded according to standard procedures and serially sectioned at 7 μm using a microtome Slides were deparaffinized, rehydrated and stained with hematoxylin-eosin (H&E) using common protocols. Digital pictures (20× magnification) were acquired with an Olympus (Germany) digital camera and then processed using an image analysis software (Image-Pro Plus 4.5 Media Cybernetics, MD). In all comparison, at least 10 embryos for each category were examined.

Acridine Orange Assay

To detect apoptotic cells in live embryos at 24 hpf, they were dechorionated and soaked in egg water containing 2 μg/ml acridine orange at 28°C for 20 min. After washing with eggs water six times 5 min each, embryos were anesthetized with tricaine (3-amino benzoic acid ethyl ester Sigma), mounted in 1% agarose and examined by Confocal Microscopy (LSM 510 Zeiss, Germany).

Mannitol Exposure

Double morphants were divided so that half of each group was maintained continuously in either normal aquarium water or in 250 mM mannitol, respectively. In experiments designed to test the ability of mannitol to reduce pre-existing edema, the fishes were treated as described and daily 10 embryos were removed from each group from 72 to 144 hpf.

Dye Filtration Experiments

A 1% solution of lysine-fixable rhodamine dextran (10,000 *M*r) was prepared in phosphate buffered saline and injected into the sinus venosus of immobilized embryos. Before injection, embryos were anaesthetized using a 0.2 mg/ml tricaine solution in egg water. All microscopy was performed on a Zeiss Axioplan.

ACKNOWLEDGMENTS

This work was supported in part by grants from 60% MIUR (2010–2011-2012), from "Associazione Amici per il Cuore" to D.Z. and in part by Fondazione CARIPLO Zebragene Grant to G.B., E.M., and R.B. P.S. is supported by DFG grant Schu 802/3-2. We thank Prof. Marco Presta for his precious scientific support.

REFERENCES

Boehm M, Bonifacino JS. 2001. Adaptins: the final recount. Mol Biol Cell 12: 2907–2920.

Boehm M, Bonifacino JS. 2002. Genetic analyses of adaptin function from yeast to mammals. Gene 286:175–186.

Bonifacino JS, Traub LM. 2003. Signals for sorting of transmembrane proteins to endosomes and lysosomes. Annu Rev Biochem 72:395–447.

Cancino J, Torrealba C, Soza A, Yuseff MI, Gravotta D, Henklein P, Rodriguez-Boulan E, Gonzalez A. 2007. Antibody to AP1B adaptor blocks biosynthetic and recycling routes of basolateral proteins at recycling endosomes. Mol Biol Cell 18:4872–4884.

Carvajal-Gonzalez JM, Gravotta D, Mattera R, Diaz F, Perez Bay A, Roman AC, Schreiner RP, Thuenauer R, Bonifacino JS, Rodriguez-Boulan E. 2012. Basolateral sorting of the coxsackie and adenovirus receptor through interaction of a canonical YXXPhi motif with the clathrin adaptors AP-1A and AP-1B. Proc Natl Acad Sci U S A 109: 3820–3825.

Cole LK, Ross LS. 2001. Apoptosis in the developing zebrafish embryo. Dev Biol 240:123–142.

Collins BM, McCoy AJ, Kent HM, Evans PR, Owen DJ. 2002. Molecular architecture and functional model of the endocytic AP2 complex. Cell 109:523–535.

Conner SD, Schmid SL. 2002. Identification of an adaptor-associated kinase, AAK1, as a regulator of clathrin-mediated endocytosis. J Cell Biol 156: 921–929.

Dressler GR, Woolf AS. 1999. Pax2 in development and renal disease. Int J Dev Biol 43:463–468.

Drummond IA, Majumdar A, Hentschel H, Elger M, Solnica-Krezel L, Schier AF, Neuhauss SC, Stemple DL, Zwartkruis F, Rangini Z, Driever W, Fishman MC. 1998. Early development of the zebrafish pronephros and analysis of mutations affecting pronephric function. Development 125:4655–4667.

Edgar RC. 2004. MUSCLE: multiple sequence alignment with high accuracy and high throughput. Nucleic Acids Res 32:1792–1797.

Eskelinen EL, Meyer C, Ohno H, von Figura K, Schu P. 2002. The polarized epithelia-specific mu 1B-adaptin complements mu 1A-deficiency in fibroblasts. EMBO Rep 3:471–477.

Farias GG, Cuitino L, Guo X, Ren X, Jarnik M, Mattera R, Bonifacino JS. 2012. Signal-mediated, AP-1/clathrin-dependent sorting of transmembrane receptors to the somatodendritic domain of hippocampal neurons. Neuron 75:810–823.

Fields IC, King SM, Shteyn E, Kang RS, Folsch H. 2010. Phosphatidylinositol 3,4,5-trisphosphate localization in recycling endosomes is necessary for AP-1B-dependent sorting in polarized epithelial cells. Mol Biol Cell 21:95–105.

Folsch H, Pypaert M, Schu P, Mellman I. 2001. Distribution and function of AP-1 clathrin adaptor complexes in polarized epithelial cells. J Cell Biol 152:595–606.

Ghosh P, Kornfeld S. 2003. AP-1 binding to sorting signals and release from clathrin-coated vesicles is regulated by phosphorylation. J Cell Biol 160:699–708.

Gilardelli CN, Pozzoli O, Sordino P, Matassi G, Cotelli F. 2004. Functional and hierarchical interactions among zebrafish vox/vent homeobox genes. Dev Dyn 230:494–508.

Glyvuk N, Tsytsyura Y, Geumann C, D'Hooge R, Huve J, Kratzke M, Baltes J, Boening D, Klingauf J, Schu P. 2010. AP-1/sigma1B-adaptin mediates endosomal synaptic vesicle recycling, learning and memory. EMBO J 29:1318–1330.

Gonzalez A, Rodriguez-Boulan E. 2009. Clathrin and AP1B: key roles in basolateral trafficking through trans-endosomal routes. FEBS Lett 583:3784–3795.

Gravotta D, Carvajal-Gonzalez JM, Mattera R, Deborde S, Banfelder JR, Bonifacino JS, Rodriguez-Boulan E. 2012. The clathrin adaptor AP-1A mediates basolateral polarity. Dev Cell 22: 811–823.

Guindon S, Gascuel O. 2003. A simple, fast, and accurate algorithm to estimate large phylogenies by maximum likelihood. Syst Biol 52:696–704.

Hase K, Nakatsu F, Ohmae M, Sugihara K, Shioda N, Takahashi D, Obata Y, Furusawa Y, Fujimura Y, Yamashita T, Fukuda S, Okamoto H, Asano M,

Yonemura S, Ohno H. 2013. AP-1B-mediated protein sorting regulates polarity and proliferation of intestinal epithelial cells in mice. Gastroenterology 145:625–635.
Heldwein EE, Macia E, Wang J, Yin HL, Kirchhausen T, Harrison SC. 2004. Crystal structure of the clathrin adaptor protein 1 core. Proc Natl Acad Sci U S A 101:14108–14113.
Hill AJ, Bello SM, Prasch AL, Peterson RE, Heideman W. 2004. Water permeability and TCDD-induced edema in zebrafish early-life stages. Toxicol Sci 78:78–87.
Hirst J, Barlow LD, Francisco GC, Sahlender DA, Seaman MN, Dacks JB, Robinson MS. 2011. The fifth adaptor protein complex. PLoS Biol 9:e1001170.
Hirst J, Irving C, Borner GH. 2013. Adaptor protein complexes AP-4 and AP-5: new players in endosomal trafficking and progressive spastic paraplegia. Traffic 14:153–164.
Jackson LP, Kelly BT, McCoy AJ, Gaffry T, James LC, Collins BM, Honing S, Evans PR, Owen DJ. 2010. A large-scale conformational change couples membrane recruitment to cargo binding in the AP2 clathrin adaptor complex. Cell 141:1220–1229.
Kimmel CB, Ballard WW, Kimmel SR, Ullmann B, Schilling TF. 1995. Stages of embryonic development of the zebrafish. Dev Dyn 203:253–310.
Korzh V, Sleptsova I, Liao J, He J, Gong Z. 1998. Expression of zebrafish bHLH genes ngn1 and nrd defines distinct stages of neural differentiation. Dev Dyn 213:92–104.
Kramer-Zucker AG, Wiessner S, Jensen AM, Drummond IA. 2005. Organization of the pronephric filtration apparatus in zebrafish requires Nephrin, Podocin and the FERM domain protein Mosaic eyes. Dev Biol 285:316–329.
Krauss M, Kukhtina V, Pechstein A, Haucke V. 2006. Stimulation of phosphatidylinositol kinase type I-mediated phosphatidylinositol (4,5)-bisphosphate synthesis by AP-2mu-cargo complexes. Proc Natl Acad Sci U S A 103:11934–11939.
Li S, Yin M, Liu S, Chen Y, Yin Y, Liu T, Zhou J. 2010. Expression of ventral diencephalon-enriched genes in zebrafish. Dev Dyn 239:3368–3379.
Liu A, Joyner AL. 2001. Early anterior/posterior patterning of the midbrain and cerebellum. Annu Rev Neurosci 24:869–896.
Majumdar A, Lun K, Brand M, Drummond IA. 2000. Zebrafish no isthmus reveals a role for pax2.1 in tubule differentiation and patterning events in the pronephric primordia. Development 127:2089–2098.
Medigeshi GR, Krikunova M, Radhakrishnan K, Wenzel D, Klingauf J, Schu P. 2008. AP-1 membrane-cytoplasm recycling regulated by mu1A-adaptin. Traffic 9:121–132.
Meyer C, Zizioli D, Lausmann S, Eskelinen EL, Hamann J, Saftig P, von Figura K, Schu P. 2000. mu1A-adaptin-deficient mice: lethality, loss of AP-1 binding and rerouting of mannose 6-phosphate receptors. EMBO J 19:2193–2203.
Montpetit A, Cote S, Brustein E, Drouin CA, Lapointe L, Boudreau M, Meloche C, Drouin R, Hudson TJ, Drapeau P, Cossette P. 2008. Disruption of AP1S1, causing a novel neurocutaneous syndrome, perturbs development of the skin and spinal cord. PLoS Genet 4: e1000296.
Mueller T, Wullimann MF. 2002. Expression domains of neuroD (nrd) in the early postembryonic zebrafish brain. Brain Res Bull 57:377–379.
Nakatsu F, Kadohira T, Gilbert DJ, Jenkins NA, Kakuta H, Copeland NG, Saito T, Ohno H. 1999. Genomic structure and chromosome mapping of the genes encoding clathrin-associated adaptor medium chains mu1A (Ap1m1) and mu1B (Ap1m2). Cytogenet Cell Genet 87:53–58.
Ohno H. 2006. Clathrin-associated adaptor protein complexes. J Cell Sci 119: 3719–3721.
Ohno H, Tomemori T, Nakatsu F, Okazaki Y, Aguilar RC, Foelsch H, Mellman I, Saito T, Shirasawa T, Bonifacino JS. 1999. Mu1B, a novel adaptor medium chain expressed in polarized epithelial cells. FEBS Lett 449:215–220.
Perez Bay AE, Schreiner R, Mazzoni F, Carvajal-Gonzalez JM, Gravotta D, Perret E, Lehmann Mantaras G, Zhu YS, Rodriguez-Boulan EJ. 2013. The kinesin KIF16B mediates apical transcytosis of transferrin receptor in AP-1B-deficient epithelia. EMBO J 32:2125–2139.
Pistocchi A, Gaudenzi G, Carra S, Bresciani E, Del Giacco L, Cotelli F. 2008. Crucial role of zebrafish prox1 in hypothalamic catecholaminergic neurons development. BMC Dev Biol 8:27.
Postlethwait JH, Yan YL, Gates MA, Horne S, Amores A, Brownlie A, Donovan A, Egan ES, Force A, Gong Z, Goutel C, Fritz A, Kelsh R, Knapik E, Liao E, Paw B, Ransom D, Singer A, Thomson M, Abduljabbar TS, Yelick P, Beier D, Joly JS, Larhammar D, Rosa F, Westerfield M, Zon LI, Johnson SL, Talbot WS. 1998. Vertebrate genome evolution and the zebrafish gene map. Nat Genet 18:345–349.
Puschel AW, Westerfield M, Dressler GR. 1992. Comparative analysis of Pax-2 protein distributions during neurulation in mice and zebrafish. Mech Dev 38: 197–208.
Radhakrishnan K, Baltes J, Creemers JW, Schu P. 2013. Trans-Golgi network morphology and sorting is regulated by prolyl-oligopeptidase-like protein PREPL and the AP-1 complex subunit mu1A. J Cell Sci 126:1155–1163.
Ricotta D, Conner SD, Schmid SL, von Figura K, Honing S. 2002. Phosphorylation of the AP2 mu subunit by AAK1 mediates high affinity binding to membrane protein sorting signals. J Cell Biol 156:791–795.
Robinson MS. 2004. Adaptable adaptors for coated vesicles. Trends Cell Biol 14: 167–174.
Schreiner R, Frindt G, Diaz F, Carvajal-Gonzalez JM, Perez Bay AE, Palmer LG, Marshansky V, Brown D, Philp NJ, Rodriguez-Boulan E. 2010. The absence of a clathrin adapter confers unique polarity essential to proximal tubule function. Kidney Int 78:382–388.
Serluca FC, Fishman MC. 2001. Pre-pattern in the pronephric kidney field of zebrafish. Development 128:2233–2241.
Takahashi D, Hase K, Kimura S, Nakatsu F, Ohmae M, Mandai Y, Sato T, Date Y, Ebisawa M, Kato T, Obata Y, Fukuda S, Kawamura YI, Dohi T, Katsuno T, Yokosuka O, Waguri S, Ohno H. 2011. The epithelia-specific membrane trafficking factor AP-1B controls gut immune homeostasis in mice. Gastroenterology 141:621–632.
Thisse C, Thisse B. 2008. High-resolution in situ hybridization to whole-mount zebrafish embryos. Nat Protoc 3:59–69.
Thompson JD, Higgins DG, Gibson TJ. 1994. CLUSTAL W: improving the sensitivity of progressive multiple sequence alignment through sequence weighting, position-specific gap penalties and weight matrix choice. Nucleic Acids Res 22:4673–4680.
Torres M, Gomez-Pardo E, Dressler GR, Gruss P. 1995. Pax-2 controls multiple steps of urogenital development. Development 121:4057–4065.
Wang E, Pennington JG, Goldenring JR, Hunziker W, Dunn KW. 2001. Brefeldin A rapidly disrupts plasma membrane polarity by blocking polar sorting in common endosomes of MDCK cells. J Cell Sci 114:3309–3321.
Wang YJ, Wang J, Sun HQ, Martinez M, Sun YX, Macia E, Kirchhausen T, Albanesi JP, Roth MG, Yin HL. 2003. Phosphatidylinositol 4 phosphate regulates targeting of clathrin adaptor AP-1 complexes to the Golgi. Cell 114:299–310.
Westerfield M. 2007. The Zebrafish book. A guide for the laboratory use of zebrafish (Danio rerio). Eugene, OR: University of Oregon Press.
Zizioli D, Forlanelli E, Guarienti M, Nicoli S, Fanzani A, Bresciani R, Borsani G, Preti A, Cotelli F, Schu P. 2010. Characterization of the AP-1 mu1A and mu1B adaptins in zebrafish (Danio rerio). Dev Dyn 239:2404–2412.
Zizioli D, Meyer C, Guhde G, Saftig P, von Figura K, Schu P. 1999. Early embryonic death of mice deficient in gamma-adaptin. J Biol Chem 274:5385–5390.